Ligand shell size effects on one- and two-photon excitation fluorescence of zwitterion functionalized gold nanoclusters

Martina Perić, Zeljka Sanader, Isabelle Russier-Antoine, Hussein Fakhouri, Franck Bertorelle, Pierre-François Brevet, Xavier Le Guével, Rodolphe Antoine, Vlasta Bonačić- Koutecký

ARTICLE

Ligand shell size effects on one- and two-photon excitation fluorescence of zwitterion functionalized gold nanoclusters

Received 00th January 20xx,
Accepted 00th January 20xx

DOI: 10.1039/x0xx00000x

Martina Perić,[a] Željka Sanader Maršić,[a] Isabelle Russier-Antoine,[b] Hussein Fakhouri,[b] Franck Bertorelle,[b] Pierre-François Brevet,[b] Xavier le Guével,[c] Rodolphe Antoine[b*] and Vlasta Bonačić-Koutecký[a,d*c]

Gold nanoclusters (Au NCs) are an emerging class of luminescent nanomaterials but still suffer from moderate photoluminescence quantum yields. Recent efforts have focused on tailoring their emission properties. Introducing zwitterionic ligands to cap the metallic kernel is an efficient approach to enhance their one-photon excitation fluorescence intensity. In this work, we extend this concept to the nonlinear optical regime, i.e. two-photon excitation fluorescence. For a proper comparison between theory and experiment, both ligand and solvent effects should be considered. The effects of explicit ligands and of aqueous solvent on the optical properties of zwitterion functionalized gold nanoclusters have been studied by performing quantum mechanics/molecular mechanics (QM/MM) simulations.

A. Introduction

In the past decade, gold nanoclusters (Au NCs)[1] have emerged as fascinating luminescent nanomaterials.[2, 3] However, the photoluminescence quantum yield (QY) of most nanoclusters is still relatively low (generally of a few percent). Recent efforts focus on tailoring the emission properties,[4] including photoluminescence (PL) intensity and emission wavelength, the two basic characteristics of fluorescence. Some strategies such as surface ligand engineering,[5-7] aggregation-induced fluorescence,[8-10] silver doping,[11-16] and ligand-shell rigidifying[17, 18] have been achieved. In particular, the surface shell rigidification permits to decrease the energy loss due to intramolecular rotations and vibrations, thus increasing the PL intensity of nanoclusters. Introducing bidentate thiol zwitterionic ligands to cap the metallic kernel is another efficient approach to rigidify the surface structure of metal nanocluster.[19] Several groups have prepared bright fluorescent nanoclusters using this strategy.[20-23] The PL intensity and emission wavelength of these nanoclusters can be easily tailored via controlling the functional groups of the zwitterionic ligands.[24] Indeed, due, to the zwiterionic form of the tails of ligands, strong intermolecular electrostatic interactions occur allowing for the formation of different ligand shells on the surface of the gold clusters.[24, 25]

[a]*Center of Excellence for Science and Technology-Integration of Mediterranean Region (STIM) at Interdisciplinary Center for Advanced Sciences and Technology (ICAST), University of Split, Poljička cesta 35, 21000 Split, Croatia.*
[b]*Institut lumière matière, UMR5306, Université Claude Bernard Lyon1-CNRS, Univ. Lyon 69622, Villeurbanne cedex, France.* rodolphe.antoine@univ-lyon1.fr
[c]*Institute for Advanced Biosciences, University of Grenoble Alpes/INSERM1209/CNRS-UMR5309, Grenoble, France.*
[d]*Chemistry Department, Humboldt University of Berlin, Brook-Taylor-Strasse 2, 12489 Berlin, Germany.* vbk@chemie.hu-berlin.de
Electronic Supplementary Information (ESI) available: [composition of AuZW nanoclusters by XPS and ESIMS analysis. Experimental optical spectra of AuZw NCs. Calculated OPA and TPA spectra obtained by TD-DFT for model clusters and by QM/MM approach for entire AuZw NCs]. See DOI: 10.1039/x0xx00000x

Although it was found that the surface of Au NCs plays a major role in fluorescence generation, several fundamental issues are still not well understood. In particular, the extent to which the ligand shell and the metal core are coupled and how this coupling modulates the emission properties remain to be clarified. Therefore, theoretical explorations of the structural and electronic properties of various nanoclusters in the ground and excited states have been reported to address the origin of the photoluminescence enhancement.[26, 27] The Aikens group investigated the geometric and electronic structural changes of gold nanoclusters upon photoexcitation using time-dependent density functional theory (TD-DFT) method.[28-30] Moreover it was also shown that the inclusion of full ligands in calculations was needed to accurately describe the experimental optical spectra.[27, 28, 31]

The combination of DFT with molecular mechanics within QM/MM approach appears to be appropriate and was recently used for structural elucidation of the clusters with explicit ligands.[32] Akola and coworkers[33, 34] used QM/MM simulations to study the influence of aqueous solvent and explicit ligands (e.g. glutathione ligands) on the structural and electronic properties of thiolate-protected $Au_{25}(SR)_{18}^-$ clusters. In this article, we show that the introduction of bidentate thiol zwitterionic ligands to cap the metallic kernel is another efficient approach to enhance nonlinear response in particular two-photon excitation fluorescence. In order to address better the ingredients responsible for their enhanced photo emission, we employ a QM/MM approach with explicit ligands. This approach permits us to address the linear and nonlinear optical regime of zwitterion functionalized gold nanoclusters (AuZw NCs) evaluating effects of ligand shell size. Optical properties including one- and two-photon absorption spectra obtained at the QM/MM level of theory are in qualitative agreement with optical measurements. Ligand shell rigidification should prevent excited state geometry relaxation through intramolecular motions, as well as through the associated non-radiative energy decay pathways. For this purpose we

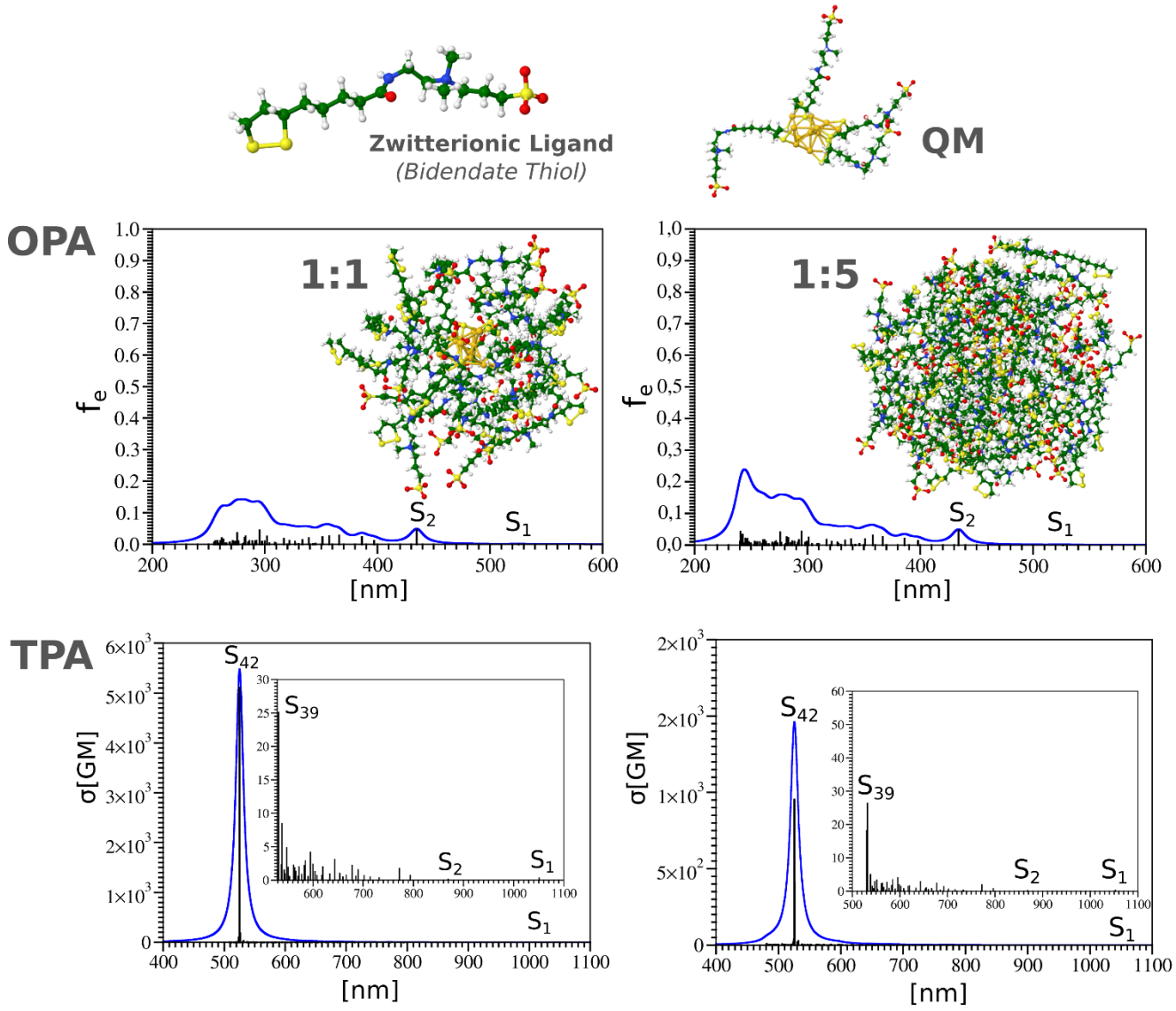

Figure 1 Comparison of OPA and TPA spectra obtained by QM/MM approach for $Au_{12}Zw_4$ (QM-TDDFT) with 1:1 and 1:5 ratio of Au/Zwitterions (MM)

investigated the influence of ligand shell size and the charge on linear and nonlinear properties of zwitterion functionalized gold nanoclusters. Also, we studied the penetration of water into AuZw NCs depending on the ligand shell sizes and their possible role as quencher for emission properties of AuZw NCs.

B. Results and discussion

Au NCs with thioctic-zwitterion ligand (Zw, $C_{15}H_{30}N_2O_4S_3$, MW=399 g·mol^{-1}, see fig. 1) were synthesized following the protocol described elsewhere.[22] As-synthesized Au NCs were characterized by X-ray photoelectron spectroscopy (XPS)[19] and by electrospray mass spectrometry (ESI-MS).[22] By controlling the initial molar ratio of Au per Zw molecules : Au:Zw, three zwitterion stabilized Au NCs with different ligand shell sizes were synthesized (named in the following as Au:Zw 1:1, Au:Zw 1:2 and Au:Zw 1:5). XPS measurements[19] show that for AuZw 1:1; 1:2 and 1:5 the ratio Au^0/Au^+ is ≈2. XPS measurements can also give a ratio between Au and sulfur atoms (~0.2). By coupling these results with mass spectrometer data, one can build AuZw clusters with a model "core" structure surrounded by a ligand shell of different size (e.g. different number of Zw molecules) (see supporting information for more details). Thus, possible molecular formula for AuZw 1:1 (≈11 kDa), AuZw 1:2 (≈ 17 kDa) and AuZw 1:5 (≈ 29 kDa) could be **$Au_{12}Zw_{22}$, $Au_{12}Zw_{37}$ and $Au_{12}Zw_{66}$** respectively. In other words, the three AuZw nanoclusters can be built with a $Au_{12}Zw_4$ subunit surrounded by 18, 33 and 62 Zw molecules in the outer shell.

Experimental optical spectra, i.e. one-photon absorption (OPA), one- and two-photon excited fluorescence, are given in supporting information (Figs. S1 and S2). One and two-photon quantum yields (1PQY and 2PQY), first hyperpolarizability values as well as two-photon absorption and excited fluorescence cross sections (TPA and TPEF) are collected in Table 1. The one-photon absorption spectra of the as-synthesized AuZw NCs are very similar and show a monotonic increase of intensity below ~500 nm. Fluorescence signals are

Table 1: Absolute magnitude of the first hyperpolarizability, two-photon absorption (TPA) and two-photon excited fluorescence cross-sections (TPEF) for AuZw clusters at 800 nm laser excitation wavelength. Of note, the measurements TPA and TPEF cross sections for AuZw 1:1 and AuZw 1:5 were not possible due to their poor photostability under laser irradiation (requiring higher concentrations for measurements as compared to HRS experiments).

AuZW cluster	Formula	1PQY (%)	Hyperpolarizability (esu)	TPA cross section (GM)	TPEF cross section (GM)	2PQY (%)
AuZw 1:1	$Au_{12}ZW_{22}$	< 0.01	$89(2).10^{-30}$	N/A	N/A	
AuZw 1:2	$Au_{12}ZW_{37}$	0.1	$146(1).10^{-30}$	N/A	N/A	
AuZW 1:5	$Au_{12}ZW_{66}$	1.4	$82(1).10^{-30}$	10000	0.5	$5\ 10^{-3}$

strongly enhanced when Zw > Au as it was previously reported.[22] Furthermore, TPEF spectra for AuZw 1:5 display two bands in the blue and red region of visible range (See Fig. S2). Note that for AuZw 1:1 and AuZw 1:2 NCs, TPEF spectra display only one band in the blue with a weak intensity (data not shown). One and two-photon quantum yields of 1.4 % and $5x10^{-3}$ % respectively are reported for AuZw 1:5 NCs. Experimentally, for AuZw 1:5, we found that the TPEF cross section at 800 nm excitation is 0.5 GM and the two-photon absorption (TPA) cross section 10000 GM. The first hyperpolarizability determined for an excitation wavelength of 800 nm for the AuZw NCs is found in the same range of the hyperpolarizability values reported for other protected gold nanoclusters.[35-37]

The important point here is that linear absorption properties are not drastically changed by changing the ligand shell size and for the AuZw NCs surrounded by the largest ligand shell (i.e. AuZw 1:5), but dramatic enhancements in the one- and two-photon excited fluorescence signals are observed.

The effects of ligand shell size on both the linear and nonlinear optical properties of zwitterion functionalized gold nanoclusters (AuZw NCs) have been investigated by performing QM/MM simulations. For the QM/MM study, the 12 gold atoms and the 4 zwitterionic ligands form the QM region. Ligands are either explicit zwitterions or modeled by S-CH_2-CH_2-CH_2-S. The outer shell, surrounded by 18 or 62 explicit Zw molecules for AuZw ratios 1:1 and 1:5, are taken into account in the MM part (see computational section for more details). TDDFT QM/MM results obtained for OPA and TPA spectra for both systems are shown in Figure 1.

OPA spectra are located between 550 and 350 nm and are in qualitative agreement with experimental findings. They are of low intensities confirming that there is no explicit metallic core with delocalized electrons. In fact, structural properties of $Au_{12}Zw_4$ are characterized by 7 Au atoms forming two tetrahedral subunits connected by central Au atom. Note that 6 Au atoms are also part of the staple motifs (cf Figure 1). Calculated OPA spectrum for $Au_{12}Zw_4$ (given in Figs. S3 and S4 in supporting information) is similar to those calculated for NCs with the full ligand shell (compare fig. 1 and fig. S3). Due to the fact that the S_1 state in OPA is located at ~525 nm, the lowest two-photon transition occurs approximately at ~1050 nm with a negligible value of cross section. The leading transitions for TPA involve ligand-core excitations. The calculations of additional TPA states give rise to S_{42} located at about 525 nm with a high value of TPA cross section. (cf Figure 1). Both OPA and TPA spectra are not dependent from the ligand shell size (compare spectra for AuZw 1:1 and 1:5) as observed experimentally for linear absorption spectra. Calculated spectra are also very similar to those obtained for $Au_{12}L_4$ with L modeled by S-CH_2-CH_2-CH_2-S (see Fig. S3) confirming that linear absorption properties of S_1 and S_2 excited states are mainly due to excitations between central and neighboring Au atoms and therefore they do not depend on the lengths of ligands.

Our findings indicate that linear absorption properties of studied systems do not depend significantly from: i) ligand size (S-CH_2-CH_2-CH_2-S vs explicit Zw ligand) and ii) ligand shell size (from 1:1 to 1:5). The question can be raised whether the charge has effect on optical properties. Therefore we introduced the positive charge (+1) placed near to central Au atom for system with modeled and explicit zwitterion ligands as show in Figures S5 and S6. The charge induces significant red shift of dominant features at experimentally accessible wavelengths. This is expected due to the lack of one electron.[38]

An origin on the effect of ligand shell size on emission properties may be rigidification effect brought by the ligand shell on the gold kernel. However, already for AuZw 1:1, the number of ligands, the steric hindrance brought by the long-chain ligands as well as strong electrostatic interactions between permanent charges of terminal zwitterions may be enough to produce a string rigidification of the gold kernel. The addition of external ligand shells with AuZw 1:2 and AuZw 1:5 might have a moderate influence on the overall rigidity. Another origin may be due to a possible quenching effect due to water penetration propensity through the ligand shell. To better address this possible quenching effect due to water penetration propensity through the ligand shell, we investigated the density of water molecules within ligated gold clusters with AuZw ratio 1:1 and 1:5. Figure 2 illustrates that penetration of water is significantly higher for 1:1 than for 1:5 AuZw ratio. This suggests that quenching effects produced by the interaction of water with the gold kernel will be less with 1:5 ratio than with 1:1 ratio for NCs and might be responsible for measured larger emissive properties for AuZw 1:5 than in the case of AuZw 1:1. Interestingly, some analogy can be found with the ligand effects on the catalytic activities of polymer-protected gold nanoclusters. Okumura and co-workers.[39-41] investigated the effects of polymer type and size, and it turned out that the polymer of low active polymer-protected gold nanoclusters inhibit the penetration of H_2O and reactants.

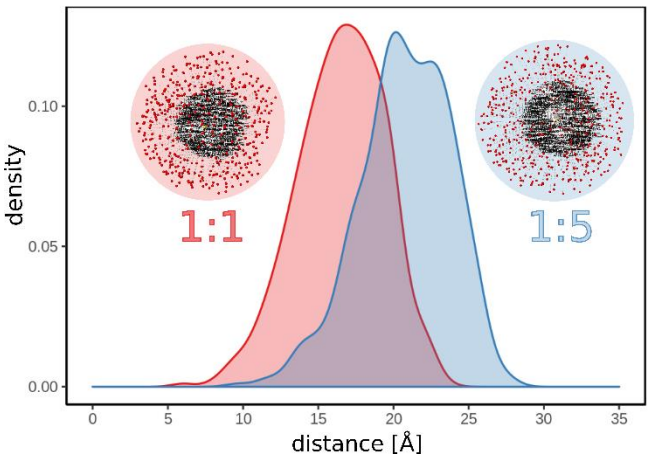

Figure 2 Density of water molecules as a function of radial distance from central Au atom within ligated gold clusters for ratio 1:1 (red) and 1:5 (blue)

C. Experimental and computational details

Experimental Details. All chemical products were purchased from Sigma Aldrich (FRANCE). **Synthesis of AuZw nanoclusters.** lipoic acid-based sulfobetaine ligand (Zw, 399 g.mol.[1]) was synthesized following the procedure described elsewhere.[42] Au NCs were prepared with different molar ratios of Au per Zw (Au:Zw)= 1:1; 1:2, and 1:5 under basic conditions in the presence of sodium borohydride as a reducing agent. Briefly, in a standard experiment for the molar ratio Au:Zw 1:5, 12.5 mmol of Zw was added to the basic mixture of 50µL of $HAuCl_4.3H_2O$ (50 mM) in 10 mL of deionized water and 10µL of NaOH (2M) under stirring for 5 min. Then, 100 µL of freshly prepared $NaBH_4$ (50 mM) was added to the solution and stirred for 15 hours. The solution changed quickly from colorless to brownish indicating the growth of Au NCs. Afterwards, the solution containing AuZw NCs was purified three times using 3kDa cut-off flters (Amicon ultra, Millipore) to remove the excess of free ligands. The pH was adjusted to 7 and the AuZw NC solution was kept refrigerated until use. **Instrumentation.** UV-vis spectra in solution were recorded using an AvaSpec-2048 fiber optic spectrometer and an AvaLight-DH-S deuterium halogen light source. Fluorescence spectra were measured using a Fluoromax-4 Horiba fluorescence spectrophotometer. The light source for the present HRS and TPA experiments was a mode-locked femtosecond Ti:sapphire laser delivering at the fundamental wavelength of 800 nm pulses with a duration of about 140 femtoseconds at a repetition rate of 76 MHz, as described in ref.[43] . Two-photon excited fluorescence measurements were performed with a customized confocal microscope (TE2000-U, Nikon Inc.) in which the excitation light entrance has been modified to allow free-space laser beam input, instead of the original optical-fiber light input. The luminescence was excited at 780 nm with a mode-locked frequency-doubled femtosecond Er-doped fiber laser (C-Fiber 780, MenloSystems GmbH), as described in ref.[44].

Computational Details. For the gold atoms the 19-e^- relativistic effective core potential (19-e^- RECP) from the Stuttgart group[45] taking into account scalar relativistic effects has been employed. For all atoms, split valence polarization atomic basis sets (SVP) have been used[46]. Coulomb-attenuated version of Becke's three-parameter non-local exchange functional together with the Lee-Yang-Parr gradient-corrected correlation functional (CAM-B3LYP)[47] have been employed to calculate optical properties. This approach has been used to determine OPA and TPA spectra (DALTON[48, 49] program) for optimized structures of Au12L14 (L= S-CH_2-CH_2-CH_2-S or zwitterionic ligand). In order to determine OPA and TPA for both systems with Au:Zw ratio 1:1 and 1:5 the two-layer quantum mechanics/molecular mechanics QM/MM approach[50] has been used. QM part includes $Au_{12}Zw_4$ (Zw= full ligand) and for the MM part the UFF force field (ref) has been employed. Polarizable embedding- quantum mechanics (PEQM) method with monopoles taken from UFF force field, implemented in Dalton package programs[48, 49] has been used within the QM/MM approach for calculation of linear and nonlinear properties. One- and two-photon OPA and TPA absorption spectra were determined employing quadratic response properties within the time-dependent density functional theory (TDDFT).[48, 49] For the calculation of TPA cross section (σ)[51], the two-photon absorption probability (δ) is needed which can be obtained from two-photon absorption transition matrices from the ground to the excited state using either single residue or double residue quadratic response procedure[52, 53]

In order to simulate penetration of water molecules in both systems with Au:Zw ratios 1:1 and 1:5, 500 neutral water molecules have been included in MM part within QM/MM approach for the optimization of geometries. In addition, we formed the model by taking into account the distances from central Au atom to each water molecule in order to obtain radial distribution of the density of water molecules using R-studio software.[54]

Conclusions

To summarize, the introduction of bidentate thiol zwitterionic ligands to cap the metallic kernel is another efficient approach to enhance nonlinear response in particular two-photon excitation fluorescence; The larger the ligand shell the higher the two-photon excitation fluorescence signal. Our QM/MM approach allowed for adequate description of key optical signatures of zwitterion functionalized gold clusters. These findings open the road for gaining insight into the origin of luminescence enhancement caused by different surface shell rigidification strategies such as introduction of bulky counter-ions or protein templating AuNCs, for which explicit templates at the molecular level are required.

Conflicts of interest

There are no conflicts to declare.

Acknowledgments

This research was partially supported by the project STIM – REI, Contract Number: KK.01.1.1.01.0003, funded by the European Union through the European Regional Development Fund – the Operational Programme Competitiveness and Cohesion 2014-2020 (KK.01.1.1.01). We would also like to acknowledge the financial support received from the French-Croatian project "International Laboratory for Nano Clusters and Biological Aging, LIA NCBA". The authors would like to thank Christophe Moulin for his help with the confocal microscope.

Notes and references

1. R. Jin, *Nanoscale*, 2010, 2, 343-362.
2. L. Y. Chen, C. W. Wang, Z. Q. Yuan and H. T. Chang, *Analytical Chemistry*, 2015, 87, 216-229.

3. H. Z. Yu, B. Rao, W. Jiang, S. Yang and M. Z. Zhu, *Coord. Chem. Rev.*, 2019, 378, 595-617.
4. X. Kang and M. Zhu, *Chemical Society Reviews*, 2019, DOI: 10.1039/c8cs00800k.
5. Z. Wu and R. Jin, *Nano Letters*, 2010, 10, 2568-2573.
6. A. Kim, C. Zeng, M. Zhou and R. Jin, *Particle & Particle Systems Characterization*, 2017, 34, 1600388.
7. Y. Lin, P. Charchar, A. J. Christofferson, M. R. Thomas, N. Todorova, M. M. Mazo, Q. Chen, J. Doutch, R. Richardson, I. Yarovsky and M. M. Stevens, *Journal of the American Chemical Society*, 2018, 140, 18217-18226.
8. Z. Luo, X. Yuan, Y. Yu, Q. Zhang, D. T. Leong, J. Y. Lee and J. Xie, *Journal of the American Chemical Society*, 2012, 134, 16662-16670.
9. N. Goswami, Q. Yao, Z. Luo, J. Li, T. Chen and J. Xie, *The Journal of Physical Chemistry Letters*, 2016, 7, 962-975.
10. B. Musnier, K. D. Wegner, C. Comby-Zerbino, V. Trouillet, M. Jourdan, I. Häusler, R. Antoine, J.-L. Coll, U. Resch-Genger and X. Le Guével, *Nanoscale*, 2019, 11, 12092-12096.
11. S. Wang, X. Meng, A. Das, T. Li, Y. Song, T. Cao, X. Zhu, M. Zhu and R. Jin, *Angewandte Chemie International Edition*, 2014, 53, 2376-2380.
12. G. Soldan, M. A. Aljuhani, M. S. Bootharaju, L. G. AbdulHalim, M. R. Parida, A.-H. Emwas, O. F. Mohammed and O. M. Bakr, *Angewandte Chemie International Edition*, 2016, 55, 5749-5753.
13. X. Le Guével, V. Trouillet, C. Spies, K. Li, T. Laaksonen, D. Auerbach, G. Jung and M. Schneider, *Nanoscale*, 2012, 4, 7624-7631.
14. D. Mishra, S. Wang, Z. Jin, Y. Xin, E. Lochner and H. Mattoussi, *Physical Chemistry Chemical Physics*, 2019, DOI: 10.1039/C9CP03723C.
15. D. Mishra, V. Lobodin, C. Zhang, F. Aldeek, E. Lochner and H. Mattoussi, *Physical Chemistry Chemical Physics*, 2018, 20, 12992-13007.
16. H. Fakhouri, M. Perić, F. Bertorelle, P. Dugourd, X. Dagany, I. Russier-Antoine, P.-F. Brevet, V. Bonačić-Koutecký and R. Antoine, *Physical Chemistry Chemical Physics*, 2019, 21, 12091-12099.
17. K. Pyo, V. D. Thanthirige, K. Kwak, P. Pandurangan, G. Ramakrishna and D. Lee, *Journal of the American Chemical Society*, 2015, 137, 8244-8250.
18. F. Bertorelle, C. Moulin, A. Soleilhac, C. Comby-Zerbino, P. Dugourd, I. Russier-Antoine, P.-F. Brevet and R. Antoine, *ChemPhysChem*, 2018, 19, 165-168.
19. X. L. Guevel, O. Tagit, C. E. Rodríguez, V. Trouillet, M. Pernia Leal and N. Hildebrandt, *Nanoscale*, 2014, 6, 8091-8099.
20. A. Yahia-Ammar, D. Sierra, F. Mérola, N. Hildebrandt and X. Le Guével, *ACS Nano*, 2016, 10, 2591-2599.
21. Y. Chen, D. M. Montana, H. Wei, J. M. Cordero, M. Schneider, X. Le Guével, O. Chen, O. T. Bruns and M. G. Bawendi, *Nano Letters*, 2017, 17, 6330-6334.
22. D. Shen, M. Henry, V. Trouillet, C. Comby-Zerbino, F. Bertorelle, L. Sancey, R. Antoine, J.-L. Coll, V. Josserand and X. L. Guével, *APL Materials*, 2017, 5, 053404.
23. F. Aldeek, M. A. H. Muhammed, G. Palui, N. Zhan and H. Mattoussi, *ACS Nano*, 2013, 7, 2509-2521.
24. E. Porret, L. Sancey, A. Martín-Serrano, M. I. Montañez, R. Seeman, A. Yahia-Ammar, H. Okuno, F. Gomez, A. Ariza, N. Hildebrandt, J.-B. Fleury, J.-L. Coll and X. Le Guével, *Chemistry of Materials*, 2017, 29, 7497-7506.
25. E. Porret, M. Jourdan, B. Gennaro, C. Comby-Zerbino, F. Bertorelle, V. Trouillet, X. Qiu, C. Zoukimian, D. Boturyn, N. Hildebrandt, R. Antoine, J.-L. Coll and X. Le Guével, *The Journal of Physical Chemistry C*, 2019, DOI: 10.1021/acs.jpcc.9b08492.
26. X.-Y. Xie, P. Xiao, X. Cao, W.-H. Fang, G. Cui and M. Dolg, *Angewandte Chemie International Edition*, 2018, 57, 9965-9969.
27. C. M. Aikens, *Accounts of Chemical Research*, 2018, 51, 3065-3073.
28. K. L. D. M. Weerawardene and C. M. Aikens, *Journal of the American Chemical Society*, 2016, 138, 11202-11210.
29. K. L. D. M. Weerawardene, E. B. Guidez and C. M. Aikens, *The Journal of Physical Chemistry C*, 2017, 121, 15416-15423.
30. R. D. Senanayake, E. B. Guidez, A. J. Neukirch, O. V. Prezhdo and C. M. Aikens, *The Journal of Physical Chemistry C*, 2018, 122, 16380-16388.
31. C. Comby-Zerbino, M. Perić, F. Bertorelle, F. Chirot, P. Dugourd, V. Bonačić-Koutecký and R. Antoine, *Nanomaterials*, 2019, 9, 457.
32. S. Banerjee, J. A. Montgomery and J. A. Gascón, *Journal of Materials Science*, 2012, 47, 7686-7692.
33. V. Rojas-Cervellera, L. Raich, J. Akola and C. Rovira, *Nanoscale*, 2017, 9, 3121-3127.
34. V. Rojas-Cervellera, C. Rovira and J. Akola, *The Journal of Physical Chemistry Letters*, 2015, 6, 3859-3865.
35. F. Bertorelle, I. Russier-Antoine, N. Calin, C. Comby-Zerbino, A. Bensalah-Ledoux, S. Guy, P. Dugourd, P.-F. Brevet, Z. Sanader, M. Krstic, V. Bonacic-Koutecky and R. Antoine, *J. Phys. Chem. Lett.*, 2017, 8, 1979-1985.
36. F. Bertorelle, I. Russier-Antoine, C. Comby-Zerbino, F. Chirot, P. Dugourd, P.-F. Brevet and R. Antoine, *ACS Omega*, 2018, 3, 15635-15642.
37. I. Russier-Antoine, F. Bertorelle, M. Vojkovic, D. Rayane, E. Salmon, C. Jonin, P. Dugourd, R. Antoine and P.-F. Brevet, *Nanoscale*, 2014, 6, 13572-13578.
38. V. Bonačić-Koutecký, J. Pittner, M. Boiron and P. Fantucci, *The Journal of Chemical Physics*, 1999, 110, 3876-3886.
39. Y. Ato, A. Hayashi, H. Koga, K. Tada, T. Kawakami, S. Yamanaka and M. Okumura, *Journal of Computational Chemistry*, 2019, 40, 222-228.
40. M. Okumura, Y. Kitagawa, T. Kawakami and M. Haruta, *Chemical Physics Letters*, 2008, 459, 133-136.
41. K. Sakata, Y. Ato, K. Tada, H. Koga, S. Yamanaka, T. Kawakami, T. Saito and M. Okumura, *Chemistry Letters*, 2016, 45, 344-346.
42. J. Park, J. Nam, N. Won, H. Jin, S. Jung, S. Jung, S.-H. Cho and S. Kim, *Advanced Functional Materials*, 2011, 21, 1558-1566.
43. I. Russier-Antoine, F. Bertorelle, N. Calin, Z. Sanader, M. Krstic, C. Comby-Zerbino, P. Dugourd, P.-F. Brevet, V. Bonacic-Koutecky and R. Antoine, *Nanoscale*, 2017, 9, 1221-1228.
44. V. Bonačić-Koutecký and R. Antoine, *Nanoscale*, 2019, 11, 12436-12448.
45. D. Andrae, U. Häußermann, M. Dolg, H. Stoll and H. Preuß, *Theoret. Chim. Acta*, 1990, 77, 123-141.
46. F. Weigend and R. Ahlrichs, *Physical Chemistry Chemical Physics*, 2005, 7, 3297-3305.
47. T. Yanai, D. P. Tew and N. C. Handy, *Chemical Physics Letters*, 2004, 393, 51-57.

48. K. Aidas, C. Angeli, K. L. Bak, V. Bakken, R. Bast, L. Boman, O. Christiansen, R. Cimiraglia, S. Coriani, P. Dahle, E. K. Dalskov, U. Ekström, T. Enevoldsen, J. J. Eriksen, P. Ettenhuber, B. Fernández, L. Ferrighi, H. Fliegl, L. Frediani, K. Hald, A. Halkier, C. Hättig, H. Heiberg, T. Helgaker, A. C. Hennum, H. Hettema, E. Hjertenæs, S. Høst, I.-M. Høyvik, M. F. Iozzi, B. Jansík, H. J. A. Jensen, D. Jonsson, P. Jørgensen, J. Kauczor, S. Kirpekar, T. Kjærgaard, W. Klopper, S. Knecht, R. Kobayashi, H. Koch, J. Kongsted, A. Krapp, K. Kristensen, A. Ligabue, O. B. Lutnæs, J. I. Melo, K. V. Mikkelsen, R. H. Myhre, C. Neiss, C. B. Nielsen, P. Norman, J. Olsen, J. M. H. Olsen, A. Osted, M. J. Packer, F. Pawlowski, T. B. Pedersen, P. F. Provasi, S. Reine, Z. Rinkevicius, T. A. Ruden, K. Ruud, V. V. Rybkin, P. Sałek, C. C. M. Samson, A. S. de Merás, T. Saue, S. P. A. Sauer, B. Schimmelpfennig, K. Sneskov, A. H. Steindal, K. O. Sylvester-Hvid, P. R. Taylor, A. M. Teale, E. I. Tellgren, D. P. Tew, A. J. Thorvaldsen, L. Thøgersen, O. Vahtras, M. A. Watson, D. J. D. Wilson, M. Ziolkowski and H. Ågren, *Wiley Interdisciplinary Reviews: Computational Molecular Science*, 2014, 4, 269-284.

49. a. m. e. s. p. Dalton, (2015), vol. Release Dalton2016.0.

50. D. Buceta, N. Busto, G. Barone, J. M. Leal, F. Domínguez, L. J. Giovanetti, F. G. Requejo, B. García and M. A. López-Quintela, *Angewandte Chemie International Edition*, 2015, 54, 7612-7616.

51. L. Frediani, Z. Rinkevicius and H. Ågren, *The Journal of Chemical Physics*, 2005, 122, 244104.

52. N. H. List, R. Zaleśny, N. A. Murugan, J. Kongsted, W. Bartkowiak and H. Ågren, *Journal of Chemical Theory and Computation*, 2015, 11, 4182-4188.

53. P. Norman, *Physical Chemistry Chemical Physics*, 2011, 13, 20519-20535.

54. *RStudio Team (2015). RStudio: Integrated Development for R. RStudio, Inc., Boston, MA URL http://www.rstudio.com/.*